

MISO Broadcast Channel with Imperfect and (Un)matched CSIT in the Frequency Domain: DoF Region and Transmission Strategies

Chenxi Hao and Bruno Clerckx

Communication and Signal Processing Group, Department of Electrical and Electronic Engineering
Imperial College London, United Kingdom

Email: {chenxi.hao10,b.clerckx}@imperial.ac.uk

Abstract—In this contribution, we focus on a frequency domain two-user Multiple-Input-Single-Output Broadcast Channel (MISO BC) where the transmitter has imperfect and (un)matched Channel State Information (CSI) of the two users in two subbands. We provide an upper-bound to the Degrees-of-Freedom (DoF) region, which is tight compared to the state of the art. By decomposing the subbands into subchannels according to the CSI feedback qualities, we interpret the DoF region as the weighted-sum of that in each subchannel. Moreover, we study the sum DoF loss when employing sub-optimal schemes, namely Frequency Division Multiple Access (FDMA), Zero-Forcing Beamforming (ZFBF) and the $S_3^{3/2}$ scheme proposed by Tandon et al. The results show that by switching among the sub-optimal strategies, we can obtain at least 80% and 66.7% of the optimal sum DoF performance for the unmatched and matched CSIT scenario respectively. ¹

I. INTRODUCTION

Transmitter side channel state information (CSIT) is crucial to the DoF performance in downlink BC, but the CSIT in practice is subject to latency and inaccuracy. Since Maddah-Ali and Tse have showed the usefulness of the delayed CSIT [1], many researches have investigated the DoF region in time domain BC with imperfect instantaneous and stale CSIT [2][3][4][5][6]. However, in practical systems like Long Term Evolution (LTE), the system performance loss is primarily due to CSI measurement and feedback inaccuracy rather than delay. Therefore, assuming the CSI arrives at the transmitter instantaneously, we are interested in the frequency domain BC where the CSI is measured and reported to the transmitter on a per-subband basis. Due to frequency selectivity, constraints on uplink overhead and user distribution in the cell, the quality of CSI reported to the transmitter varies across users and subbands.

The work in [5] has solved the problem when two scheduled users report their CSI on two different subbands (alternating between $I_1 I_2 = NP$ and PN^2) by proposing the $S_3^{3/2}$ scheme, achieving optimal sum DoF $\frac{3}{2}$. But what if the feedback is imperfect? Literature [7] was the first work investigating this issue. A novel transmission strategy integrating Maddah-Ali and Tse (MAT) scheme, ZFBF and FDMA is proposed

¹This work was partially supported by the Seventh Framework Programme for Research of the European Commission under grant number HARP-318489.

² I_i is the CSIT state of user i , it is perfect (P), delayed (D) or none (N).

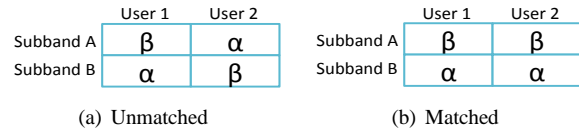


Fig. 1: Two-subband based frequency correlated BC.

considering a specific two-subband based scenario shown in Figure 1(a). However, the DoF region found in [7] is in fact suboptimal and has been improved recently by the scheme proposed in [6], inspired by the $S_3^{3/2}$ scheme.

A. Main Contributions

In this paper, we first continue the study in [7] and [6] by giving a converse in Section II, showing the optimality of the achievable scheme in [6] for the unmatched CSIT. The optimal bound and achievable scheme for the scenario with matched CSIT (see Figure 1(b)) are also addressed. Besides, we provide a weighted-sum interpretation of the DoF region.

Second, we analyze the achievability of the schemes proposed in [7] and [6] in Section III. The origins of the DoF loss in [7] is clarified.

Third, in Section IV, rather than applying a complicated optimal strategy in both unmatched or matched cases, we switch among FDMA, ZFBF and $S_3^{3/2}$ in order to achieve a certain percentage of the optimal sum DoF performance. Interestingly, the results show that the optimal scheme can be replaced by the suboptimal switching strategy if we aim at achieving at least 80% and 66.7% of the optimal performance in the unmatched and matched scenario, respectively.

B. Notations

Bold lower letters stand for vectors whereas a symbol not in bold font represents a scalar. $(\cdot)^T$ and $(\cdot)^H$ represent the transpose and conjugate transpose of a matrix or vector respectively. \mathbf{h}^\perp denotes the orthogonal space of the channel vector \mathbf{h} . $\mathcal{E}[\cdot]$ refers to the expectation of a random variable, vector or matrix. $\|\cdot\|$ is the norm of a vector. $f(P) \sim P^B$ corresponds to $\lim_{P \rightarrow \infty} \frac{\log f(P)}{\log P} = B$, where P is the SNR throughout the paper and logarithms are in base 2. For a V_j that is a function of the index j , we denote $V_{j_1}^{j_2}$ as the set $\{V_{j_1}, V_{j_1+1}, \dots, V_{j_2}\}$ if $j_1 \leq j_2$. Otherwise, $V_{j_1}^{j_2}$ is an empty set.

C. System Model

1) *Frequency domain two-user MISO BC*: We consider one 2-antenna transmitter and two single-antenna users. The transmit signal is denoted as \mathbf{s}_j , subject to a per-subband power constraint $\mathcal{E}[\|\mathbf{s}_j\|^2] \sim P$. The observations at user 1 and 2, y_j and z_j respectively, are given by

$$y_j = \mathbf{h}_j^H \mathbf{s}_j + \epsilon_{j1}, \quad z_j = \mathbf{g}_j^H \mathbf{s}_j + \epsilon_{j2}, \quad j=A, B \quad (1)$$

where ϵ_{j1} and ϵ_{j2} are unit power AWGN noise. \mathbf{h}_A and \mathbf{h}_B , both with \mathbf{I}_2 covariance matrix, are the CSI of user 1 in *subband A* and *B* respectively. \mathbf{g}_A and \mathbf{g}_B are those of user 2. The CSI are i.i.d across users and subbands.

2) *CSI Feedback Model*: Classically, in Frequency Division Duplexing (FDD), each user estimates their CSI in the specified subband using pilot and the estimated CSI is quantized and reported to the transmitter via a rate-limited link. In Time Division Duplexing (TDD), CSI is measured on the uplink and used in the downlink assuming channel reciprocity. We assume a general setup (valid for both FDD and TDD) where the transmitter obtains the CSI instantaneously, but with imperfectness, due to the estimation error and/or finite rate in the feedback link.

Denoting the imperfect CSI in *subband j* as $\hat{\mathbf{h}}_j$ and $\hat{\mathbf{g}}_j$, the CSI of user 1 and user 2 can be respectively modeled as $\mathbf{h}_j = \hat{\mathbf{h}}_j + \tilde{\mathbf{h}}_j$ and $\mathbf{g}_j = \hat{\mathbf{g}}_j + \tilde{\mathbf{g}}_j$, where $\tilde{\mathbf{h}}_j$ and $\tilde{\mathbf{g}}_j$ are the error vectors, respectively with the covariance matrix $\mathbb{E}[\tilde{\mathbf{h}}_j \tilde{\mathbf{h}}_j^H] = \sigma_{j1}^2 \mathbf{I}_2$ and $\mathbb{E}[\tilde{\mathbf{g}}_j \tilde{\mathbf{g}}_j^H] = \sigma_{j2}^2 \mathbf{I}_2$. $\hat{\mathbf{h}}_j$ and $\hat{\mathbf{g}}_j$ are respectively independent of $\tilde{\mathbf{h}}_j$ and $\tilde{\mathbf{g}}_j$. The norm of $\hat{\mathbf{h}}_j$ and $\hat{\mathbf{g}}_j$ scale as P^0 at infinite SNR.

To investigate the impact of the imperfect CSIT on the *DoF* region, we assume that the variance of the error exponentially scales with SNR, namely $\sigma_{j1}^2 \sim P^{-a_j}$ and $\sigma_{j2}^2 \sim P^{-b_j}$. a_j and b_j are respectively interpreted as the quality of CSIT of user 1 and user 2 in subband j , given as follows

$$a_j = \lim_{P \rightarrow \infty} -\frac{\log \sigma_{j1}^2}{\log P}, \quad b_j = \lim_{P \rightarrow \infty} -\frac{\log \sigma_{j2}^2}{\log P}, \quad (2)$$

where P is the SNR throughout the paper since the variance of the AWGN noise has been normalized.

Figure 1(a) shows the scenario with unmatched (alternating) CSIT, where $a_1 = b_2 = \beta$ and $a_2 = b_1 = \alpha$. Without loss of generality, we assume that $\beta \geq \alpha$. Figure 1(b) illustrates the scenario with matched CSIT, namely $a_1 = b_1 = \beta$ and $a_2 = b_2 = \alpha$.

β and α vary within the range of $[0, 1]$. $\beta = 1$ (resp. $\alpha = 1$) is equivalent to perfect CSIT because the full *DoF* region can be achieved by simply doing ZFBF. $\beta = 0$ (resp. $\alpha = 0$) means that the variance of the CSI error scales as P^0 , such that the imperfect CSIT cannot benefit the *DoF* when doing ZFBF.

3) *DoF Definition*: The *DoF* is defined on a per-channel-use basis as

$$d_k \triangleq \lim_{P \rightarrow \infty} \frac{R_k}{r \log P}, \quad k = 1, 2, \quad (3)$$

where R_k is the rate achieved by user k over r channel uses.

II. OUTER-BOUND OF THE DOF REGION

Theorem 1. *The outer-bound of the DoF region in the frequency correlated BC with imperfect CSIT (for both unmatched and matched scenario) is specified by*

$$d_1 + d_2 \leq 1 + \frac{\beta + \alpha}{2}, \quad d_1 \leq 1, \quad d_2 \leq 1. \quad (4)$$

A. Proof of Theorem 1

Let us first revisit the converse in previous literatures. In [8], the *DoF* region in the BC without CSIT is upper-bounded by considering one user's observation is degraded compared to the other's. In the BC with delayed CSIT [1][2][3], the outer-bound is obtained through the genie-aided model where one user's observation is provided to the other, thus establishing a physically degraded BC to remove the delayed CSIT.

However, in this contribution, those methods are not adopted since the transmitter does not have delayed CSIT and the BC with imperfect CSIT cannot be simply considered as a degraded BC. Instead, we follow the assumption in [9]: We first consider that user 2 knows the message intended to user 1, which leads to an outer-bound denoted by \mathbb{D}_1 ; Then by assuming that user 1 knows user 2's desired message, we can have another region \mathbb{D}_2 . The final *DoF* outer-bound results from the intersection of them, i.e. $\mathbb{D} = \mathbb{D}_1 \cap \mathbb{D}_2$. This assumption is somehow consistent with the outer-bound given by Theorem 5 in [10], which is used to find a tight upper bound on the weighted sum rate in vector Gaussian BC (Section 4.1, [11]).

We assume that the transmission lasts for n subbands ($n \rightarrow \infty$), half of which are *subband A* and the rest are *subband B*. The set of the observations of user 1 and user 2 from *subband j* to j_2 are defined as $Y_{j_1}^{j_2}$ and $Z_{j_1}^{j_2}$ respectively. The set of the imperfect CSI of user 1 and 2 are respectively represented as $\hat{\mathcal{H}}_1^n$ and $\hat{\mathcal{G}}_1^n$ and they are known at both transmitter side and receiver side. $\tilde{\mathcal{H}}_1^n$ and $\tilde{\mathcal{G}}_1^n$ are the set of errors vectors which are only available at user 1 and user 2 respectively. The transmit signal \mathbf{s}_j in subband j is any sequence of $(2^{nR_1}, 2^{nR_2}, n)$ as a function of W_1 (user 1's messages), W_2 (user 2's messages) and $\hat{\mathcal{H}}_1^n, \hat{\mathcal{G}}_1^n$.

Considering that user 2 knows W_1 , we derive \mathbb{D}_1 as follows

$$nR_1 \leq I(W_1; Y_1^n | \hat{\mathcal{H}}_1^n, \hat{\mathcal{G}}_1^n, \tilde{\mathcal{H}}_1^n) \quad (5)$$

$$\begin{aligned} &= \underbrace{h(Y_1^n | \hat{\mathcal{H}}_1^n, \hat{\mathcal{G}}_1^n, \tilde{\mathcal{H}}_1^n)}_{\leq h(Y_1^n) \leq n \log P} - h(Y_1^n | W_1, \hat{\mathcal{H}}_1^n, \hat{\mathcal{G}}_1^n, \tilde{\mathcal{H}}_1^n) \\ &\leq n \log P - h(Y_1^n | W_1, \hat{\mathcal{H}}_1^n, \hat{\mathcal{G}}_1^n, \tilde{\mathcal{H}}_1^n), \end{aligned} \quad (6)$$

$$nR_2 \leq I(W_2; Z_1^n | \hat{\mathcal{H}}_1^n, \hat{\mathcal{G}}_1^n, \tilde{\mathcal{G}}_1^n, W_1) \quad (7)$$

$$\begin{aligned} &= h(Z_1^n | \hat{\mathcal{H}}_1^n, \hat{\mathcal{G}}_1^n, \tilde{\mathcal{G}}_1^n, W_1) - \underbrace{h(Z_1^n | \hat{\mathcal{H}}_1^n, \hat{\mathcal{G}}_1^n, \tilde{\mathcal{G}}_1^n, W_1, W_2)}_{\leq n \log P} \\ &\leq h(Z_1^n | \hat{\mathcal{H}}_1^n, \hat{\mathcal{G}}_1^n, \tilde{\mathcal{G}}_1^n, W_1). \end{aligned} \quad (8)$$

Hence,

$$\begin{aligned} n(R_1 + R_2) &\leq n \log P + h(Z_1^n | \hat{\mathcal{H}}_1^n, \hat{\mathcal{G}}_1^n, \tilde{\mathcal{G}}_1^n, W_1) \\ &\quad - h(Y_1^n | \hat{\mathcal{H}}_1^n, \hat{\mathcal{G}}_1^n, \tilde{\mathcal{H}}_1^n, W_1) \end{aligned}$$

$$\begin{aligned}
&=n\log P+h(Z_1^n|\hat{\mathcal{H}}_1^n,\hat{\mathcal{G}}_1^n,\tilde{\mathcal{G}}_1^n,\tilde{\mathcal{H}}_1^n,W_1) \\
&\quad -h(Y_1^n|\hat{\mathcal{H}}_1^n,\hat{\mathcal{G}}_1^n,\tilde{\mathcal{G}}_1^n,\tilde{\mathcal{H}}_1^n,W_1). \tag{9}
\end{aligned}$$

(9) follows the fact that Z_1^n is independent of $\tilde{\mathcal{H}}_1^n$ conditioned on $\{\hat{\mathcal{H}}_1^n,\hat{\mathcal{G}}_1^n,\tilde{\mathcal{G}}_1^n,W_1\}$, and Y_1^n is independent of $\tilde{\mathcal{G}}_1^n$ conditioned on $\{\hat{\mathcal{H}}_1^n,\hat{\mathcal{G}}_1^n,\tilde{\mathcal{H}}_1^n,W_1\}$. For convenience, we denote $\Omega\triangleq\{\hat{\mathcal{H}}_1^n,\hat{\mathcal{G}}_1^n,\tilde{\mathcal{G}}_1^n,\tilde{\mathcal{H}}_1^n,W_1\}$. Consequently,

$$\begin{aligned}
n(R_1+R_2)&=n\log P+h(Z_1^n|\Omega)-h(Y_1^n|\Omega) \\
&=n\log P+\sum_{j=1}^n\{h(Z_j|\Omega,Y_1^{j-1},Z_{j+1}^n) \\
&\quad -h(Y_j|\Omega,Y_1^{j-1},Z_{j+1}^n)\}. \tag{10}
\end{aligned}$$

(10) is similar to equation (44) in [9]. We provide the derivation in the Appendix.

In the following, we introduce a new notation as

$$\begin{aligned}
\{T_j,\tilde{Q}\}&\triangleq\{\Omega,Y_1^{j-1},Z_{j+1}^n\}, \\
T_j&\triangleq\{Y_1^{j-1},Z_{j+1}^n,W_1,\hat{\mathcal{H}}_1^n,\hat{\mathcal{G}}_1^n\}, \quad \tilde{Q}\triangleq\{\tilde{\mathcal{H}}_1^n,\tilde{\mathcal{G}}_1^n\}.
\end{aligned}$$

Next, we aim at maximizing each term in the summation of (10) following the footsteps in [2]. We note

$$\begin{aligned}
h(Z_j|T_j,\tilde{Q})-h(Y_j|T_j,\tilde{Q}) \\
\leq\max_{P_{T_j},P_{s_j|T_j}}\{h(Z_j|T_j,\tilde{Q})-h(Y_j|T_j,\tilde{Q})\}, \tag{11}
\end{aligned}$$

where the maximizations are taken over all the possible joint distributions of $P(T_j,s_j)$. We write

$$\begin{aligned}
(11)&\leq\max_{P_{T_j}}\mathcal{E}_{T_j}\{\max_{P_{s_j|T_j}}h(Z_j|T_j=T^*,\tilde{Q})-h(Y_j|T_j=T^*,\tilde{Q})\} \\
&=\max_{P_{T_j}}\mathcal{E}_{T_j}\{\max_{P_{s_j|T_j}}\mathcal{E}_{\tilde{Q}|T_j}[h(Z_j|T_j=T^*,\tilde{Q}=\tilde{Q}^*) \\
&\quad -h(Y_j|T_j=T^*,\tilde{Q}=\tilde{Q}^*)]\} \\
&=\max_{P_{T_j}}\mathcal{E}_{T_j}\{\max_{P_{s_j|T_j}}\mathcal{E}_{\tilde{Q}}[h(\mathbf{g}_j^H\mathbf{s}_j+\epsilon_{j2}|T_j=T^*) \\
&\quad -h(\mathbf{h}_j^H\mathbf{s}_j+\epsilon_{j1}|T_j=T^*)]\} \\
&=\max_{P_{T_j}}\mathcal{E}_{T_j}\{\max_{\mathbf{K}\succeq\mathbf{0},0\leq\text{tr}(\mathbf{K})\leq P}\mathcal{E}_{\tilde{Q}}[h(\mathbf{g}_j^H\mathbf{s}_j+\epsilon_{j2}|T_j=T^*) \\
&\quad -h(\mathbf{h}_j^H\mathbf{s}_j+\epsilon_{j1}|T_j=T^*)]\} \\
&\leq\max_{\tilde{Q}}\mathcal{E}_{\tilde{Q}}\{\max_{\mathbf{K}\succeq\mathbf{0},0\leq\text{tr}(\mathbf{K})\leq P}\mathcal{E}_{\tilde{Q}}[\log(1+\mathbf{g}_j^H\mathbf{K}\mathbf{g}_j) \\
&\quad -\log(1+\mathbf{h}_j^H\mathbf{K}\mathbf{h}_j)]\}, \tag{12}
\end{aligned}$$

where $Q=\hat{Q}+\tilde{Q}$ with $\hat{Q}\triangleq\{\hat{\mathcal{H}}_1^n,\hat{\mathcal{G}}_1^n\}$ is the channel state of both users and \mathbf{K} is the covariance matrix of \mathbf{s}_j . (12) is derived according to the fact 1) $\mathbf{s}_j\rightarrow T_j\rightarrow\mathbf{g}_j$ forms a Markov chain so that \mathbf{g}_j is independent of \mathbf{s}_j conditioned on T_j ; 2) A Gaussian distributed \mathbf{s}_j conditioned on T_j is the optimal solution to the maximization of the weighted difference in (12), based on the proof of Corollary 6 in [11].

Using Lemma 1 in [2], we can respectively upper- and lower-bound the first and second terms in (12) as

$$\mathcal{E}_{\tilde{Q}}\log(1+\mathbf{g}_j^H\mathbf{K}\mathbf{g}_j)\leq\log(1+\lambda_1\mathcal{E}[\|\tilde{\mathbf{g}}_j\|^2])+O(1), \tag{13}$$

$$\mathcal{E}_{\tilde{Q}}\log(1+\mathbf{h}_j^H\mathbf{K}\mathbf{h}_j)\geq\log(1+e^{-\gamma}\lambda_1\mathcal{E}[\|\tilde{\mathbf{h}}_j\|^2])+O(1), \tag{14}$$

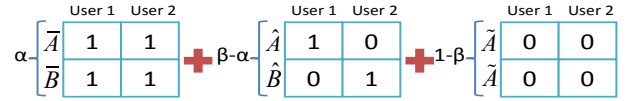


Fig. 2: Channel decomposition for the unmatched case.

where γ is constant, λ_1 is the largest eigen-value of the covariance matrix \mathbf{K} . Substituting the terms in (12) with (13) and (14), we can upper-bound (10) by

$$n(R_1+R_2)\leq n\log P+\sum_{j=1}^n\log\frac{1+\lambda_1\mathcal{E}[\|\tilde{\mathbf{g}}_j\|^2]}{1+e^{-\gamma}\lambda_1\mathcal{E}[\|\tilde{\mathbf{h}}_j\|^2]}. \tag{15}$$

As *subband A* and *B* respectively take half of the n subbands, replacing $\mathcal{E}[\|\tilde{\mathbf{g}}_j\|^2]$, $\mathcal{E}[\|\tilde{\mathbf{h}}_j\|^2]$ with the corresponding values, we obtain

$$\mathbb{D}_1:d_1+d_2\leq 1+\frac{\alpha+\beta}{2}, \tag{16}$$

Switching the role of each user, the same formula is obtained for \mathbb{D}_2 . (4) holds for both unmatched and matched case. \square

B. A Weighted-Sum DoF Interpretation

In this part, we decompose the channel in each subband by making use of the intuition that the imperfect CSIT with error variance $P^{-\alpha}$ can be considered as perfect for α ($0\leq\alpha\leq 1$) channel use (i.e. the transmit power is reduced to $\mathcal{E}[\|\mathbf{s}\|^2]\leq P^\alpha$). We can see this by simply sending one private message per user using ZFBF precoding and with power P^α . Since $\mathcal{E}[\|\mathbf{h}_j^H\hat{\mathbf{h}}_j^\perp\|^2]\sim P^{-\alpha}$ and $\mathcal{E}[\|\mathbf{g}_j^H\hat{\mathbf{g}}_j^\perp\|^2]\sim P^{-\alpha}$, both users can recover their private message only subject to noise. Therefore, the rate $\alpha\log P$ is achieved per user. As only α channel has been used, full *DoF* region is obtained according to (3). This is in fact a generalization of the fact that full *DoF* region can be obtained if the error in CSIT is scaled as SNR^{-1} [2].

Therefore, we decompose the subbands into subchannels as follows (see Figure 2):

- \tilde{A} , \tilde{B} : no CSIT, each with channel use $1-\beta$;
- \hat{A} (\hat{B}): perfect CSIT of user 1 (2), with channel use $\beta-\alpha$;
- \bar{A} , \bar{B} : perfect CSIT of both users, with channel use α .

The *DoF* region in *subbands A* and *B* can be obtained as the weighted-sum of the regions in each subchannel.

Subchannel \tilde{A} and *\tilde{B}* can be categorized as the BC with no CSIT, whose *DoF* region has been studied in [8]. The outer-bound (denoted as \tilde{D}) is given by

$$\mathcal{D}^{\tilde{A}}=\mathcal{D}^{\tilde{B}}=\tilde{D}:d_1+d_2\leq 1. \tag{17}$$

Subchannel \bar{A} and *\bar{B}* are the BC with perfect CSIT of both users, the outer-bound is expressed (via a notation \bar{D}) as

$$\mathcal{D}^{\bar{A}}=\mathcal{D}^{\bar{B}}=\bar{D}:d_1\leq 1,d_2\leq 1. \tag{18}$$

However, *subchannel \hat{A}* and *\hat{B}* have an alternating CSIT setting with two states [5]: $I_1I_2=PN$ and $I_1I_2=NP$. The optimal *DoF* region has been found in [5] as

$$(\mathcal{D}^{\hat{A}}+\mathcal{D}^{\hat{B}})/2=\hat{D}:d_1+d_2\leq 1.5,d_1\leq 1,d_2\leq 1. \tag{19}$$

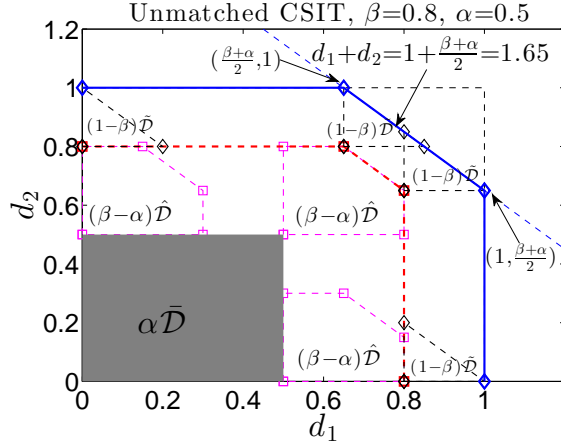


Fig. 3: Composing \mathcal{D}_u with $\beta=0.8$ and $\alpha=0.5$

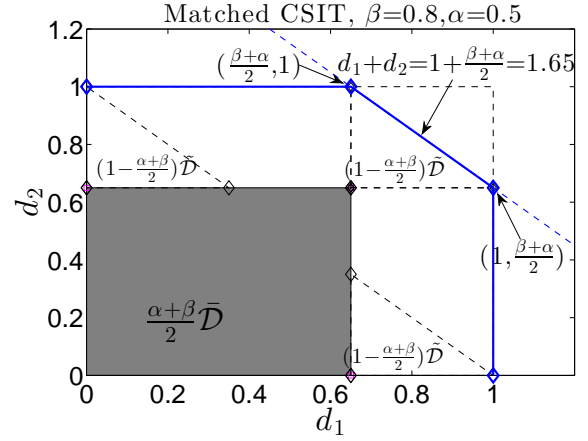


Fig. 4: Composing \mathcal{D}_m with $\beta=0.8$ and $\alpha=0.5$

Consequently, by combining (17), (18), (19), we can obtain a weighted-sum representation of the *DoF* region as

$$\mathcal{D}_u = (1 - \beta)\tilde{\mathcal{D}} + (\beta - \alpha)\hat{\mathcal{D}} + \alpha\bar{\mathcal{D}}. \quad (20)$$

Similarly, *subband A* and *B* with matched CSIT can be decomposed as

- \tilde{A} , \tilde{B} : no CSIT, each with channel use $1-\beta$ and $1-\alpha$;
- \hat{A} , \hat{B} : perfect CSIT of both users, with channel use β and α respectively.

The weighted sum form of the outer-bound \mathcal{D}_m is given by

$$\mathcal{D}_m = \left(1 - \frac{\beta + \alpha}{2}\right)\tilde{\mathcal{D}} + \frac{\beta + \alpha}{2}\bar{\mathcal{D}}. \quad (21)$$

Figure 3 and 4 respectively illustrate the composition of \mathcal{D}_u and \mathcal{D}_m . In Figure 3, the grey square area depicts the region $\alpha\bar{\mathcal{D}}$. All the valid points inside $\alpha\bar{\mathcal{D}}$ are expanded to a magenta polygon representing $(\beta-\alpha)\hat{\mathcal{D}}$. This expansion results in the bound shown by the dashed red curve with square points. Then, every point on this bound is further expanded to a black triangle area referring to $(1-\beta)\tilde{\mathcal{D}}$. Outlining all the expanded area, we can obtain \mathcal{D}_u bounded by the solid blue curve with diamond points. It results in inequalities (4). \mathcal{D}_m is made up similarly and illustrated in Figure 4, resulting in (4) as well.

The outer-bound shown in Figure 3 is consistent with the achievable region in [6], therefore showing that the bound in Theorem 1 is the optimal *DoF* region. The outer-bound illustrated in Figure 4 is also an optimal bound, its achievability will be discussed in Section III-C.

Remark: The imperfect CSIT setting can be viewed as the alternating CSIT configuration in [5], when the weight in front of each term is interpreted as the fraction of the state PP, NP/PN or NN. Also, the value $\frac{\alpha+\beta}{2}$ in (4) stands for the average quality of CSIT of a user, corresponding to the parameter λ_P in *Remark 1* and *2* in [5], which represents the fraction of channel use when the CSIT of a user is available.

III. ACHIEVABILITY ANALYSIS

In this section, we aim at identifying the shortness of the scheme in [7] in the unmatched case by comparing it with [6] and identifying the optimal scheme for the matched case.

subband A	subband B	Power	Rate (logP)
$x_{c,A}$	$x_{c,B}$	$P - P^\beta$	$1 - \beta$
u_A	v_B	$P^\alpha/2$	α
u_0	u_0	$(P^\beta - P^\alpha)/2$	$\beta - \alpha$
v_A	u_B	$P^\beta/2$	β

TABLE I: Power and rate allocation in the optimal scheme.

A. Unmatched Case: Revisiting the Optimal Scheme in [6]

The transmit signals in *subband A* and *B* are expressed as

$$\mathbf{s}_A = [x_{c,A}, 0]^T + [\hat{\mathbf{g}}_A^\perp, \hat{\mathbf{g}}_A][u_A, u_0]^T + \hat{\mathbf{h}}_A^\perp v_A, \quad (22)$$

$$\mathbf{s}_B = [x_{c,B}, 0]^T + [\hat{\mathbf{h}}_B^\perp, \hat{\mathbf{h}}_B][v_B, u_0]^T + \hat{\mathbf{g}}_B^\perp u_B. \quad (23)$$

$x_{c,A}$ and $x_{c,B}$ are common messages that should be decoded by both users (but could be intended to user 1 and user 2 respectively or exclusively to user 1 or user 2). u_A , u_0 and u_B are symbols sent to user 1, while v_A and v_B are symbols to user 2. The rate and power allocation are shown in Table I, resulting in the received signals at each user (y_A and y_B for user 1 and z_A and z_B for user 2) as

$$y_A = \underbrace{h_{A,1}^* x_{c,A}}_P + \underbrace{\mathbf{h}_A^H \hat{\mathbf{g}}_A^\perp u_A}_{P^\alpha} + \underbrace{\mathbf{h}_A^H \hat{\mathbf{g}}_A u_0}_{P^\beta} + \underbrace{\mathbf{h}_A^H \hat{\mathbf{h}}_A^\perp v_A}_{P^0}, \quad (24)$$

$$z_A = \underbrace{g_{A,1}^* x_{c,A}}_P + \underbrace{\mathbf{g}_A^H \hat{\mathbf{g}}_A^\perp u_A}_{P^0} + \underbrace{\mathbf{g}_A^H \hat{\mathbf{g}}_A u_0}_{P^\beta} + \underbrace{\mathbf{g}_A^H \hat{\mathbf{h}}_A^\perp v_A}_{P^\beta}, \quad (25)$$

$$y_B = \underbrace{h_{B,1}^* x_{c,B}}_P + \underbrace{\mathbf{h}_B^H \hat{\mathbf{h}}_B^\perp v_B}_{P^0} + \underbrace{\mathbf{h}_B^H \hat{\mathbf{h}}_B u_0}_{P^\beta} + \underbrace{\mathbf{h}_B^H \hat{\mathbf{g}}_B^\perp u_B}_{P^\beta}, \quad (26)$$

$$z_B = \underbrace{g_{B,1}^* x_{c,B}}_P + \underbrace{\mathbf{g}_B^H \hat{\mathbf{h}}_B^\perp v_B}_{P^\alpha} + \underbrace{\mathbf{g}_B^H \hat{\mathbf{h}}_B u_0}_{P^\beta} + \underbrace{\mathbf{g}_B^H \hat{\mathbf{g}}_B^\perp u_B}_{P^0}, \quad (27)$$

From (24) to (27) (ignoring the noise terms), $x_{c,A}$ and $x_{c,B}$ are first decoded by treating all the other terms as noise. Afterwards, user 1 decodes u_0 and u_A from y_A using Successive Interference Cancellation (SIC). With the knowledge of u_0 , u_B can be obtained from y_B . Similarly, user 2 decodes u_0 and v_B from z_B via SIC. v_A can be decoded from z_A by eliminating u_0 . The sum *DoF* therefore is $d_\Sigma^{\text{opt}} = 1 + \frac{\beta + \alpha}{2}$.

B. Unmatched Case: Shortness of the Scheme Proposed in [7]

The transmit signals in *subband A* and *B* are expressed as

$$\mathbf{s}_A = [x_{c,A}, 0]^T + [\mu_A, 0]^T + [\hat{\mathbf{h}}_A^\perp, \hat{\mathbf{h}}_A][v_{A1}, v_{A2}]^T + \hat{\mathbf{g}}_A^\perp u_A, \quad (28)$$

$$\mathbf{s}_B = [x_{c,B}, 0]^T + [\mu_B, 0]^T + [\hat{\mathbf{g}}_B^\perp, \hat{\mathbf{g}}_B][u_{B1}, u_{B2}]^T + \hat{\mathbf{h}}_B^\perp v_B, \quad (29)$$

where the private symbols u_A, v_{A1}, u_{B1} and v_B are precoded and transmitted with the power and rate similar to u_A, v_A, u_B and v_B in (22) and (23) respectively.

Besides, v_{A2} and u_{B2} , generated with rate $(\beta - \alpha)\log P$ similar to u_0 , are respectively overheard by user 1 in *subband A* and by user 2 in *subband B*, thus leading to the requirement of transmitting $\mu = v_{A2} + u_{B2}$ to enable the decoding of other private symbols. μ is split into μ_A and μ_B and multicast via an extra $\beta - \alpha$ channel use. However, in the optimal scheme, u_0 is the only symbol causing interference at receiver 2 in *subband A* and is simply removed after retransmission in *subband B*.

To sum up, the scheme in [7] employs $2\beta + \beta - \alpha$ channel use to transmit six private symbols (i.e. $v_{A1}, v_{A2}, u_A, u_{B1}, u_{B2}, v_B$), while the optimal scheme sends five private symbols (i.e. u_A, v_B, u_0, v_A, u_B) in 2β channel use. Their sum *DoF* are respectively expressed as (regardless of $x_{c,A}$ and $x_{c,B}$)

$$d_\Sigma^{\text{sub}} = \frac{2\beta + 2\alpha + 2(\beta - \alpha)}{3\beta - \alpha} = \frac{4\alpha + 4(\beta - \alpha)}{2\alpha + 3(\beta - \alpha)}, \quad (30)$$

$$d_\Sigma^{\text{opt}} = \frac{2\beta + 2\alpha + (\beta - \alpha)}{2\beta} = \frac{4\alpha + 3(\beta - \alpha)}{2\alpha + 2(\beta - \alpha)}. \quad (31)$$

(30) and (31) provide an explicit interpretation of how the channel resources have been used. More precisely, we can see the optimal scheme is an integration of ZFBF and $S_3^{3/2}$ in [5] while the scheme in [7] combines ZFBF with MAT. Specifically, similarly to the weighted sum in (20), both schemes employ α channel use to achieve the region \bar{D} . \bar{D} corresponds to the optimal region with perfect CSIT of both users and can be simply achieved by ZFBF. However, over the $\beta - \alpha$ channel use where the CSIT state alternates between *subchannel A* and *B*, the optimal scheme achieves $1.5(\beta - \alpha)\log P$ sum rate, consistent with \hat{D} , outperforming the scheme in [7] (with $\frac{4}{3}(\beta - \alpha)\log P$). Hence, the shortness of the scheme in [7] lies in the sub-optimality of MAT in *subchannel A* and *B*.

C. Matched Case

The region shown in Figure 4 can be achieved by transmitting the signals in each subband as

$$\mathbf{s}_i = \underbrace{[x_{c,i}, 0]^T}_{P-Pj} + \underbrace{\hat{\mathbf{g}}_i^\perp u_i}_{Pj/2} + \underbrace{\hat{\mathbf{h}}_i^\perp v_i}_{Pj/2}, \quad (i, j) = (A, \beta), (B, \alpha). \quad (32)$$

$x_{c,i}$ is decoded first at each user with rate $(1-j)\log P$ in *subband i*. Afterwards, due to partial ZFBF, the private symbols u_i and v_i can be respectively decoded with rate $j\log P$ at user 1 and user 2.

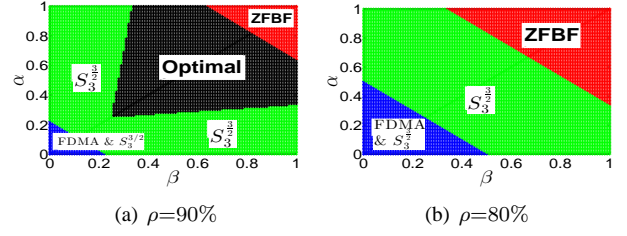


Fig. 5: Unmatched case, switching among FDMA, ZFBF and $S_3^{3/2}$.

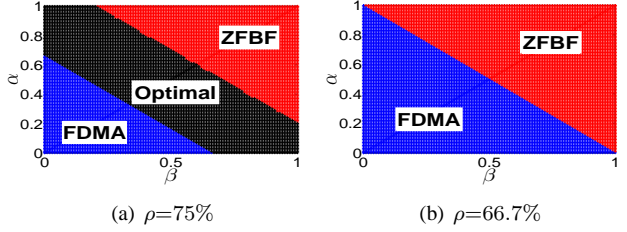


Fig. 6: Matched case, switching among FDMA and ZFBF.

IV. SWITCHING AMONG SUB-OPTIMAL STRATEGIES

As the optimal schemes discussed in Section III-A and III-C operate as an integration of FDMA, ZFBF and $S_3^{3/2}$ (in unmatched case), we will evaluate the sum *DoF* performance of sub-optimal (and less complex) transmission strategies.

A. Sub-optimal Strategies

1) *FDMA*: The sum *DoF* is $d_\Sigma^F = 1$, resulted from simply sending $x_{c,i}$ ($i=A, B$) in (22), (23) and (32) with full power.

2) *ZFBF*: The transmission boils down to ZFBF if only v_i and u_i ($i=A, B$) are sent with full power P . The received signal are respectively $y_i = \mathbf{h}_i^H \hat{\mathbf{g}}_i^\perp u_i + \mathbf{h}_i^H \hat{\mathbf{h}}_i^\perp v_i + \epsilon_1$ and $z_i = \mathbf{g}_i^H \hat{\mathbf{h}}_i^\perp v_i + \mathbf{g}_i^H \hat{\mathbf{g}}_i^\perp u_i + \epsilon_2$ at user 1 and 2, where the second terms are residual interferences with covariance $P\mathcal{E}[|\hat{\mathbf{h}}_i|^2]$ and $P\mathcal{E}[|\hat{\mathbf{g}}_i|^2]$, causing rate loss. Hence, for both unmatched and matched CSIT scenario, the sum *DoF* is $d_\Sigma^Z = \beta + \alpha$.

3) $S_3^{3/2}$: For the unmatched case, if only u_0, v_A and u_B are transmitted using the full power, the transmission boils down to $S_3^{3/2}$ in [5]. Since the qualities of $\hat{\mathbf{h}}_A^\perp$ and $\hat{\mathbf{g}}_B^\perp$ are β , u_0 is decoded with rate $\beta\log P$ by user 1 from y_A and user 2 from z_B . As a consequence, u_B and v_A are respectively obtained with rate $\log P$ from y_B and z_A . Hence, the sum *DoF* is $d_\Sigma^S = 1 + \frac{\beta}{2}$.

B. Numerical Results

Next, for all possible values of β and α , we take the max sum *DoF* performance over the aforementioned sub-optimal strategies. If the max sum *DoF* can achieve at least ρ (expressed in %) of the optimal result, the complicated optimal strategy is replaced by the sub-optimal one. Figure 5 and 6 illustrate the selection results for the unmatched and matched case respectively.

In Figure 5(a), nearly an half of the (β, α) -grid is covered by the optimal scheme when $\rho=90\%$. ZFBF has distinguished performance when (β, α) approach 1, because the CSIT works

well in rejecting the interference potentially overheard by users. $S_3^{3/2}$ scheme occupies the corners where β and α have relatively large discrepancy, as one user's rate is significantly limited in each subband if ZFBF is conducted. Both FDMA and $S_3^{3/2}$ can achieve above 90% of the optimal sum DoF performance when $\beta+\alpha \leq 0.2$.

Figure 5(b) displays an interesting result, namely that the best transmission strategy out of three covers all the possible pairs of (β, α) when the target is decreased to 80%. In other words, the best strategy among the 3 sub-optimal strategies can achieve at least 80% of the optimal sum DoF performance as

$$\max(d_{\Sigma}^F, d_{\Sigma}^Z, d_{\Sigma}^S) \geq 0.8 \times d_{\Sigma}^{opt}, \forall \beta, \alpha \in [0, 1]. \quad (33)$$

(33) can be derived by thoroughly comparing d_{Σ}^F , d_{Σ}^Z and d_{Σ}^S for different values of (β, α) . For the matched case, a similar observation results from Figure 6 as

$$\max(d_{\Sigma}^F, d_{\Sigma}^Z) \geq 2/3 \times d_{\Sigma}^{opt}, \forall \beta, \alpha \in [0, 1]. \quad (34)$$

V. CONCLUSION

In this contribution, we derive the outer-bound of the DoF region in (unmatched and matched) frequency correlated scenario introduced in [7], thus showing the optimality of the achievable DoF bound found in [6]. The bound is interpreted as a weighted sum of the DoF bound achieved by FDMA, ZFBF and $S_3^{3/2}$ in [5]. The origin of the sub-optimality of the scheme in [7] is clarified.

We have evaluated the sum DoF performance of simple sub-optimal transmission schemes (FDMA, ZFBF or $S_3^{3/2}$) for specific values of (β, α) . The results show that for the unmatched CSIT scenario, the optimal scheme proposed in [6] can be avoided if we aim at achieving 80% of the optimal sum DoF performance. In the matched CSIT scenario, the optimal scheme can be replaced by FDMA or ZFBF provided that the level of achievement is lower than 66.7%.

ACKNOWLEDGEMENT

We acknowledge fruitful discussions on the Proof of Theorem 1 with our colleague Borzoo Rassouli.

APPENDIX-PROOF OF (10)

To obtain (10), firstly we introduce

$$\Phi_j = h(Z_j^{n-j+1} | \Omega, Y_1^{j-1}, Z_{n-j+2}^n) - h(Y_j^{n-j+1} | \Omega, Y_1^{j-1}, Z_{n-j+2}^n), \text{ for } j \leq \lfloor \frac{n+1}{2} \rfloor, \quad (35)$$

$$\Theta_j = h(Z_j | \Omega, Y_1^{j-1}, Z_{j+1}^n) - h(Y_j | \Omega, Y_1^{j-1}, Z_{j+1}^n). \quad (36)$$

The last two terms in (10) can be rewritten as

$$\Phi_1 = \sum_{j=1}^n \Theta_j. \quad (37)$$

(37) can be obtained by summing the following recursive formulas and removing the identical terms

$$\Phi_j = \Theta_j + \Theta_{n-j+1} + \Phi_{j+1}, \text{ for } j \leq \lfloor \frac{n+1}{2} \rfloor - 1, \quad (38)$$

$$\Phi_{\lfloor \frac{n+1}{2} \rfloor} = \begin{cases} \Theta_{\lfloor \frac{n+1}{2} \rfloor} + \Theta_{\lfloor \frac{n+1}{2} \rfloor + 1}, & \text{if } n \text{ is even,} \\ \Theta_{\lfloor \frac{n+1}{2} \rfloor}, & \text{if } n \text{ is odd.} \end{cases} \quad (39)$$

(38) originates from the following derivations

$$\begin{aligned} & h(Z_j^{n-j+1} | \Omega, Y_1^{j-1}, Z_{n-j+2}^n) - h(Y_j^{n-j+1} | \Omega, Y_1^{j-1}, Z_{n-j+2}^n) \\ &= h(Z_j | \Omega, Y_1^{j-1}, Z_{j+1}^n) + h(Z_{j+1}^{n-j+1} | \Omega, Y_1^{j-1}, Z_{n-j+2}^n) \\ & \quad - h(Y_{n-j+1} | \Omega, Y_1^{n-j}, Z_{n-j+2}^n) - h(Y_j^{n-j} | \Omega, Y_1^{j-1}, Z_{n-j+2}^n) \\ &= h(Z_j | \Omega, Y_1^{j-1}, Z_{j+1}^n) + h(Z_{j+1}^{n-j+1} | \Omega, Y_1^{n-j}, Z_{n-j+2}^n) \\ & \quad + I(Z_{j+1}^{n-j+1}; Y_j^{n-j} | \Omega, Y_1^{j-1}, Z_{n-j+2}^n) \\ & \quad - h(Y_{n-j+1} | \Omega, Y_1^{n-j}, Z_{n-j+2}^n) - h(Y_j^{n-j} | \Omega, Y_1^{j-1}, Z_{j+1}^n) \\ & \quad - I(Y_j^{n-j}; Z_{j+1}^{n-j+1} | \Omega, Y_1^{j-1}, Z_{n-j+2}^n) \\ &= h(Z_j | \Omega, Y_1^{j-1}, Z_{j+1}^n) + h(Z_{n-j+1} | \Omega, Y_1^{n-j}, Z_{n-j+2}^n) \\ & \quad + h(Z_{j+1}^{n-j} | \Omega, Y_1^{n-j}, Z_{n-j+1}^n) \\ & \quad - h(Y_{n-j+1} | \Omega, Y_1^{n-j}, Z_{n-j+2}^n) - h(Y_j | \Omega, Y_1^{j-1}, Z_{j+1}^n) \\ & \quad - h(Y_{j+1}^{n-j} | \Omega, Y_1^j, Z_{j+1}^n) \\ &= \Theta_j + \Theta_{n-j+1} \\ & \quad + h(Z_{j+1}^{n-j} | \Omega, Y_1^j, Z_{n-j+1}^n) - I(Z_{j+1}^{n-j}; Y_{j+1}^{n-j} | \Omega, Y_1^j, Z_{n-j+1}^n) \\ & \quad - h(Y_{j+1}^{n-j} | \Omega, Y_1^j, Z_{n-j+1}^n) + I(Y_{j+1}^{n-j}; Z_{j+1}^{n-j} | \Omega, Y_1^j, Z_{n-j+1}^n) \\ &= \Theta_j + \Theta_{n-j+1} + \Phi_{j+1}. \end{aligned} \quad (40)$$

Note that we learn that (37) is known as Csiszár Sum Identity [12] after we work out the derivation.

REFERENCES

- [1] M. Maddah-Ali and D. Tse, "Completely stale transmitter channel state information is still very useful," *IEEE Trans. Inf. Theory*, vol. 58, no. 7, pp. 4418–4431, 2012.
- [2] S. Yang, M. Kobayashi, D. Gesbert, and X. Yi, "Degrees of freedom of time correlated miso broadcast channel with delayed csit," *IEEE Trans. Inf. Theory*, vol. 59, no. 1, pp. 315–328, 2013.
- [3] T. Gou and S. Jafar, "Optimal use of current and outdated channel state information: Degrees of freedom of the miso bc with mixed csit," *IEEE Comms. Letters*, vol. 16, no. 7, pp. 1084–1087, July 2012.
- [4] J. Chen and P. Elia, "Can imperfect delayed csit be as useful as perfect delayed csit? dof analysis and constructions for the bc," in *Communication, Control, and Computing (Allerton), 2012 50th Annual Allerton Conference on*, 2012, pp. 1254–1261.
- [5] R. Tandon, S. Jafar, S. Shamai Shitz, and H. Poor, "On the synergistic benefits of alternating csit for the miso broadcast channel," *IEEE Trans. Inf. Theory*, vol. 59, no. 7, pp. 4106–4128, 2013.
- [6] J. Chen and P. Elia, "Optimal dof region of the two-user miso-bc with general alternating csit," available on arXiv:1303.4352, 2013.
- [7] C. Hao and B. Clerckx, "Imperfect and unmatched csit is still useful for the frequency correlated miso broadcast channel," in *IEEE ICC 2013*, Budapest, Hungary, Jun. 2013, available on arXiv:1302.6521.
- [8] C. Huang, S. Jafar, S. Shamai, and S. Vishwanath, "On degrees of freedom region of mimo networks without channel state information at transmitters," *IEEE Trans. Inf. Theory*, vol. 58, no. 2, pp. 849–857, Feb. 2012.
- [9] A. Lapidoth, S. Shamai, and M. A. Wigger, "On the capacity of fading mimo broadcast channels with imperfect transmitter side-information," available on arXiv: 0605079, 2006.
- [10] J. Korner and K. Marton, "General broadcast channels with degraded message sets," *IEEE Trans. Inf. Theory*, vol. 23, no. 1, pp. 60–64, Jan 1977.
- [11] T. Liu and P. Viswanath, "An extremal inequality motivated by multiterminal information-theoretic problems," *IEEE Trans. Inf. Theory*, vol. 53, no. 5, pp. 1839–1851, 2007.
- [12] A. E. Gamal and Y.-H. Kim, *Network Information Theory*. Cambridge University Press, 2012.